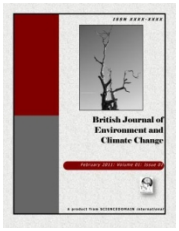

British Journal of Environment & Climate Change
3(1): 86-102, 2013

SCIENCEDOMAIN *international*
www.sciencedomain.org

Relative Efficiency of Surface Energy Partitioning Over Different Land Covers

Jiachuan Yang[1], Zhi-Hua Wang[1*] and T. –W. Lee[2]

[1]School of Sustainable Engineering and the Built Environment, Arizona State University, Tempe, AZ 85287, USA.
[2]School for Engineering of Matter, Transport and Energy, Arizona State University, Tempe, AZ 85287, USA.

Authors' contributions

This work was carried out in collaboration among all authors. Author JY performed the data analysis and wrote the first draft of the manuscript. Author ZHW designed the study, managed data collection and supervised the study. Authors ZHW and TWL proofread and finalized the manuscript. All authors read and approved the final manuscript.

Research Article

Received 16th January 2013
Accepted 16th March 2013
Published 10th April 2013

ABSTRACT

Aims: In this paper, we aim to assess different parameterization schemes for quantifying the surface energy portioning process, in particular, the latent and sensible heat fluxes, and their applicability to various surface cover types.
Study Design: This study intercompares theoretical models that predict the relative efficiency of the latent heat (evapotranspiration) with respect to the sensible heat flux. Model predictions are compared with field measurements over surface covers with different physical characteristics and soil water availability.
Place and Duration of Study: This study was carried out at the Arizona State University, Tempe, AZ, between August 2012 and December 2012.
Methodology: Three theoretical models for prediction of the relative efficiency of the latent heat were investigated, based on the lumped heat transfer (Priestley), the linear stability analysis (LSA) and the maximum entropy principle (MEP), respectively. Model predictions were compared against field measurements over three different land cover types, viz. water, grassland and suburban surfaces. An explicit moisture availability parameter β is incorporated in the MEP model, to facilitate direct comparison against the LSA and field measurements. Standard post-processing and quality control were applied

**Corresponding author: Email: zhwang@asu.edu;*

to field measured turbulent fluxes using the eddy-covariance (EC) technique. To be consistent with the premise of all theoretical models, diurnal series of sensible and latent heat fluxes were filtered such that only data points under convective conditions were selected.

Results: Among all three models, the application of Priestley model is restricted to saturated land surfaces, and generally overestimates the relative efficiency of the latent heat for water-limited surfaces. The LSA and MEP models predict similar β ranges, i.e., 0.05-0.3 in summer and 0.1-0.7 in winter over suburban area, and 0.1 to 0.5 over lake surface. Over vegetated surfaces, the MEP model predicts a reasonable β range around unity by taking transpiration into consideration, while the LSA model consistently underestimated the relative efficiency.

Conclusion: Moisture availability plays an essential role in regulating the surface energy partitioning process. The introduction of the moisture availability parameter enables versatile theoretical models for latent heat (and evapotranspiration) predictions over a wide range of land cover types. This study provides a physical insight into the thermodynamics mechanism governing the surface energy balance, and the potential to develop novel surface energy parameterization schemes based on the concept of relative efficiency. The MEP model is found to have the greatest potential in terms of future theoretical model development.

Keywords: relative efficiency; surface energy partitioning; Bowen Ratio; land cover; evapotranspiration; land-atmospheric interactions.

1. INTRODUCTION

Observational data and model simulations indicate that our globe is undergoing an unprecedented change of climate patterns, in response to increasing concentrations of greenhouse gases in the atmosphere [1]. As a consequence, we have seen, and will continue to see more frequent occurrence of extreme meteorological and climatic events, such as flooding, droughts, hurricanes, etc., [2,3,4]. These changes of climatic patterns have significant impacts on the integrated Earth system, including geophysics, ecosystems, hydrology and atmospheric dynamics. One of the key physical components of the integrated Earth system is the transfer of heat and water fluxes across the land-atmosphere interface, coupled through the terrestrial evapotranspiration process [5,6,7]. Partitioning of solar energy at the land surface provides lower boundary conditions for the atmospheric dynamics of energy and water cycles, and dictates the land-atmospheric interactions [8,9]. Energy balance for an infinitesimally thin surface layer can be written as:

$$R_n = H + LE + G \tag{1}$$

where $R_n = S^{\downarrow} + L^{\downarrow} - S^{\uparrow} - L^{\uparrow}$ is the net radiation with S and L denoting shortwave and longwave radiative components respectively; downward and upward arrows denote the down welling and upwelling components respectively; H is the sensible heat flux; LE is the latent heat flux; and G is the ground heat flux (measured at the land surface).

Individual heat flux terms on the right-hand side of equation (1) have their own significance in different geophysical, meteorological and hydrological processes. The latent heat LE is directly related to the hydrological cycle through the evapotranspiration process, which in turn affects processes such as cloud forming and moisture exchange. The sensible heat H

affects surface heating and drying, the structure of air temperature in the boundary layer, and the dynamics and thermodynamics of the lower troposphere. The ground heat *G* determines the soil thermal profile and geochemical reactions of solutes. Thus the efficiency of dissipating the available radiative energy into these dissipative fluxes is important in determining dynamics and thermodynamics of the integrated soil-vegetation-atmosphere-climate system.

Turbulent, i.e. sensible and latent, heat fluxes of the surface energy balance (SEB) system have been routinely observed at selected locations using eddy covariance (EC) towers. However, the deployment of EC towers is usually constrained by practical difficulties, e.g. logistics and maintenance. In addition, flux tower measurements have limited representative elementary area (REA) or the so-called "footprint", resulting in discrepancies in comparison with numerical modeling due to the scale variability [10,11]. For measurements or mapping of heat fluxes at relatively large scales, remote sensing techniques are advantageous in terms of large spatial coverage but susceptible to their indirect nature of measurements. Alternatively, numerical approaches have been developed using land surface temperature (LST), vegetation indices (VI) and soil moisture or other directly sensed variables to estimate the turbulent fluxes based on empirical relations [12,13,14], flux retrieval models [15,16,17], or physical parameterization schemes [18,19,20].

An alternative group of methods to parameterize turbulent fluxes is to build intrinsic relations, here referred to as relative efficiencies, among flux terms in the SEB. In this paper, relative efficiency of a heat flux is defined as the ratio of the flux to the sensible heat flux *H*. The beauty of relative-efficiency-based approaches is that they usually admit simple theoretical derivations based on basic physical laws of heat transfer and thermodynamics constraints. This class of approaches is also computationally more economic than the EC technique by imbedding physical processes of surface energy partitioning in theoretical formulations of relative efficiency coefficients. Historically, the concept of relative efficiency has been adopted to parameterize turbulent heat fluxes arising from the land surface, a prominent example being the Bowen ratio method [21]. Priestly [22] derived relative efficiencies of the ground and latent heat with respect to the sensible heat, as functions of the air-soil interface temperature and properties of the contacting media. More recently, Wang and Bras [23,24] developed numerical models for relative efficiencies based on the maximum entropy production (MEP) theory and the second law of thermodynamics. Bateni and Entekhabi [25] applied linear stability analysis (LSA) to calculate the relative efficiencies of *LE*, *G* and longwave radiation, by introducing LST perturbations to the SEB equation and quantifying the relative rate of energy dissipation to restore the thermodynamic equilibrium. In all these approaches, it was found that LST contains the signature of the partitioning of available solar radiation at the land surface. To date these models have been independently tested and evaluated against field measurements, while an intercomparison among them is still absent. In this study, we carry out an intercomparison among these mechanistic models, with a focus on the relative efficiency of the latent heat with respect to *H* (i.e. *LE*/*H*, or the reciprocal of the conventional Bowen ratio). Field measurements over various land covers were collected to evaluate different model performance.

2. METHODOLOGY

2.1 Theoretical Models

In this study, the classical method [22], the LSA model [25] and the MEP theory [23,24] were selected to represent the family of methods using the concept of relative efficiency. The principles, assumptions and results of the three methods are discussed below. Detailed descriptions of these approaches can be found in original manuscripts.

In Priestley model, the soil-atmosphere continuum is divided into two separate one dimensional (1D) semi-infinite columns by the interface, where heat transfer is dominated by diffusion. Heat is transferred through the soil-atmospheric interface at the rate governed by the temperature difference and effective diffusivity. By assuming horizontal homogeneity and small diurnal variation, the relative efficiency over a *saturated* surface is given by:

$$\frac{LE}{H} \equiv \frac{1}{Bo} = \frac{L_v}{c_p}\left(\frac{\partial q_s^*}{\partial T}\right)\Bigg|_{T=T_S} \tag{2}$$

where Bo is the Bowen ratio; L_V is the latent heat of vaporization for water; c_p is the specific heat of air; and T_s is the land surface temperature. The saturated specific humidity q_s^* in Eq. (2) is given by:

$$q_s^*(T) = \frac{\varepsilon e_s^*(T)}{p} \tag{3}$$

where ε = 0.622is the ratio of the specific gas constant of dry air to that of water vapor; p is the atmospheric pressure; and $e_s^*(T)$ is the saturated vapor pressure given by the Clausius-Clapeyron equation:

$$e_s^*(T) = e_0 \exp\left[\frac{L_v}{R_v}\left(\frac{1}{T_0} - \frac{1}{T}\right)\right]. \tag{4}$$

where T_0 and e_0 are the reference temperature and vapor pressure, respectively (usually taken as T_0 = 298.15 K and e_0 = 3617 Pa); and R_V = 461.5 J/kg•K is the specific gas constant of water vapor.

The LSA model adopts the well-known force-restore method [26,27] to approximate the subsurface heat transfer. The following assumptions are used in the fore-restore method: (a) the ground heat flux has a strong diurnal behavior; and (b) soil thermal properties are invariant with depth. *LE* and *H* are estimated using bulk resistance formulations in the model. Surface temperature T_s and air temperature T_a are treated as two independent variables, where higher order terms of T_s are linearized using Taylor expansion. The relative efficiency of latent heat is given by [25]:

$$\frac{LE}{H} = \beta\frac{\Delta}{\gamma} \tag{5}$$

where $\Delta = de_s^*/dT$ is the slope of the saturated vapor pressure curve; $\gamma = c_p p/0.622L_v$ is the psychometric constant; and$\beta$is the moisture availability parameter: β= 0 for completely dry surface and 1 for the saturated surface.

In the LSA model, computations of both Δ and γ are based on the atmospheric temperature, with land surface temperature as the controlling parameter of perturbation analysis. For liquid water surface varying from -50ºC to 102ºC, the Goff-Gratch equation is used here for vapor pressure [28,29]:

$$\begin{aligned} Log_{10}e_s^* = & -7.90298(373.16/T-1)+5.02808Log_{10}(373.16/T) \\ & -1.3816\times10^{-7}\left[10^{11.344(1-T/373.16)}-1\right] \\ & +8.1328\times10^{-3}\left[10^{-3.49149(373.16/T-1)}-1\right]+Log_{10}(1013.246) \end{aligned} \quad (6)$$

Comparing Eqs. (2) and (5), it is found that Priestley and the LSA models have similar functional forms due to the usage of similar bulk transfer mechanism for estimating *LE* and *H* in both models. The computation for e_s^* is different, and is given by Eqs. (4) and (6) for Priestley and the LSA models, respectively. Besides, Priestley model is based on surface temperature while the LSA model is based on air temperature.

In the MEP model, Wang and Bras [24] considered the condition where a time-varying source of heat due to solar radiation is present at the interface (i.e. the land surface) between two semi-infinite soil-atmosphere columns. Available energy at the surface will be dissipated by heat fluxes entering the two columns according to the thermodynamic constraint. As postulated by the MEP theory, among all attainable thermodynamic states, the system will be driven to the state where a maximum rate of entropy production is achieved [30,31,32]. Thus the MEP theory serves as a general thermodynamic limit towards which complex and non-equilibrium systems will evolve. The original formulation for the relative efficiency between latent and sensible heat derived from the MEP theory is given by [24]:

$$\frac{LE}{H}=6\left(\sqrt{1+\frac{11}{36}\sigma}-1\right) \quad (7)$$

where σ is an implicit moisture stress parameter: σ = 0 for dry soils and $\sigma = \Delta/\gamma$ for saturated soils. To explicitly introduce the soil moisture parameter β(same as the one in Eq.(5)) into the MEP formulation, Eq. (7) can be slightly rearranged as:

$$\frac{LE}{H}=6\left(\sqrt{1+\frac{11}{36}\beta\frac{\Delta}{\gamma}}-1\right) \quad (8)$$

Equation (8) facilitates direct comparison between the LSA and the MEP model predictions. Note that the computation of Δ/γ in the MEP model is based on the LST rather than the atmospheric temperature in the LSA model. For bare soils, the LST can be measured at the soil surface, leading Eq. (8) for prediction of the latent heat associated with the evaporation process. For vegetated land surface, on the other hand, the MEP model can be separately applied to quantify the transpiration process, leading to the formulation identical to Eq. (8) with Δ/γcomputed using effective leaf temperature.

In the three approaches discussed above, Priestley model applies to saturated land surfaces, while the actual water availability is accounted in the LSA and MEP models. For water surfaces, SEB is further complicated by the direct penetration of solar radiation into

water surface layer, as well as the variation of surface radiative property with solar zenith angles. As a remedy, the MEP theory is modified such that the SEB equation accounts only for the dissipation of longwave radiative energy while the shortwave component is assumed to be in equilibrium states during a diurnal cycle (Wang, private communication).

2.2 Field Measurements

To evaluate the theoretical methods of relative efficiency discussed above, three EC datasets over different land covers were collected in this study, namely, the grassland, the lake and the suburban surfaces, respectively. For the lake dataset, EC systems were installed near shore in a shallow part of the Lake Geneva (Switzerland) about 4 m deep. Four sets of sensors were arranged in a vertical array to measure the meteorological data at the height of 1.66 m, 2.31 m, 2.96 m and 3.61 m, respectively. Detailed information can be found in Vercauteren et al. [33,34]. For the grassland dataset, EC tower was installed over a dense short grass field near Princeton campus with a sampling rate of 10 Hz [35,36]. In addition, sensing instruments were deployed for continuously monitoring of a suburban area at Princeton campus, which consist of a wireless network of 12 meteorological stations and an EC station on a rooftop sampling at 20 Hz frequency [20,37]. The land cover characteristics and detailed instrumentation at each site are summarized in Table 1.

Table 1. Land cover characteristics and instrumentation for all sites

	Suburban	**Lake**	**Grassland**
Land cover type	Mix of buildings, roads, parking lots and vegetation	Water without significant aquatic vegetation	Short and dense grass
Measurement period	Continuous since Summer 2009	August to October 2006	Continuous since 2008
Radiation	Hukseflux 4-component net-radiation sensor NR01	Kipp & Zonen NR-Lite	Hukseflux 4-component net-radiation sensor NR01
Air temperature and humidity	Vaisala HMP45C	LICOR LI-7500	Vaisala HMP45C
Wind	Campbell scientific CSAT3, Young R.M. wind monitor	Campbell Scientific CSAT3, Young R.M. Wind Monitor	Campbell Scientific CSAT3
Pressure	LICOR LI-7500	LICOR LI-7500	LICOR LI-7500

High frequency EC data were post-processed using standard techniques including linear detrending, Wilczak coordinate rotation [38] and Webb's correction [39], using an integral time of 30 minutes. In addition, only daytime data points under convective conditions were selected for subsequent analysis, since Priestley and LSA models were derived based on the unstable atmospheric condition. Under convective conditions, the surface layer is dominated by buoyancy to generate strong turbulent mixing. Over the lake surface, field measurements show that the air temperature can exceed the surface temperature around noon, known as the oasis effect [40]. The oasis effect leads to downwelling sensible heat flux; and data points within this period need to be filtered. Fig. 1 illustrates typical time intervals (shaded) in measured diurnal time series that are selected for analysis over water

and land surfaces, respectively. For each diurnal cycle, mean values of the selected time period were calculated and used for subsequent analysis.

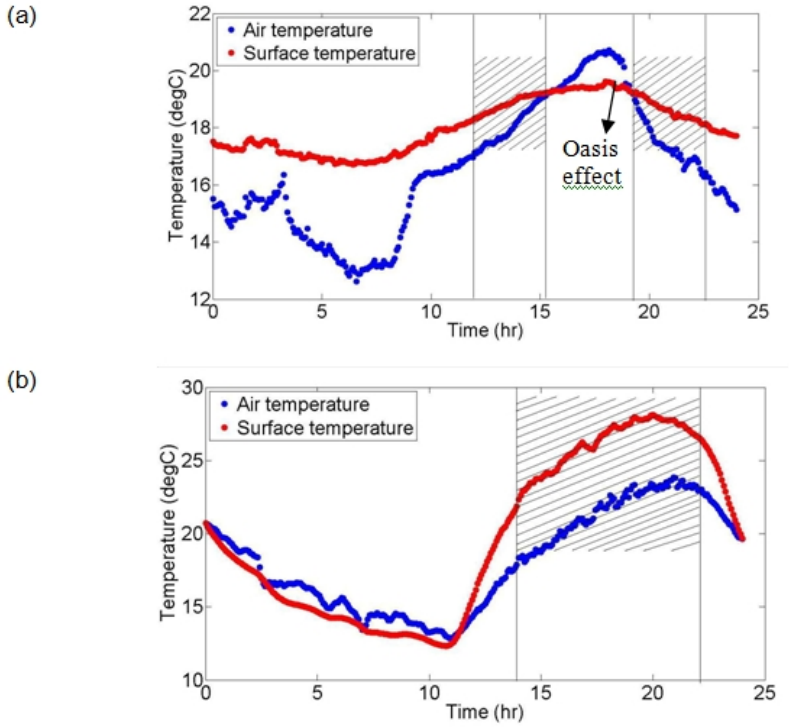

Fig. 1.Diurnal temperature variation and selected periods (shaded) under convective conditions for subsequent analysis over (a) water (lake), and (b) land (vegetated or impervious) surfaces

3. RESULTS AND DISCUSSION

3.1 Intercomparison among Theoretical Models

We first carried out intercomparison of theoretical models to identify possible similarities and differences among them. As shown in Fig. 2, in general, all models predict the same trend of the relative efficiency of latent heat flux (1/*Bo*) as increasing with the scaling temperature. The surface water availability parameter β quantitatively dictates the evolutional trend of the relative efficiency with temperature: the drier the surface, the less model sensitivity to temperature variation. When β = 1, i.e. the surface is fully saturated, model predictions by the LSA and Priestley model are nearly identical, as shown in Fig. 2(a). Deviation between the two models for the saturated surface is caused by the usage of Clausius-Clapeyron relation (Eq. (4)) or the corrected Goff-Gratch equation (Eq. (6)) in computing saturated vapor pressure. Note that the parameter β can also be incorporated into Priestley model to reflect the soil water availability scaling from 0 to 1, which will result in the prediction by Priestley model very close to that of the LSA model. Given the similarity between Priestley and LSA models, for brevity, we will focus on the comparison of the LSA and MEP models for subsequent discussion of the effect of surface water availability. In addition, Fig. 2(b) shows that predictions by the MEP model are consistently lower than that of Priestley (as

well as the LSA) model. This discrepancy is essentially due to the inherent difference in the underlying mechanistic parameterization schemes associated with formulations of turbulent heat transfer, namely, the bulk transfer approach in Priestley and LSA models in contrast to the Monin-Obukhov similarity theory (MOST) in the MEP model.

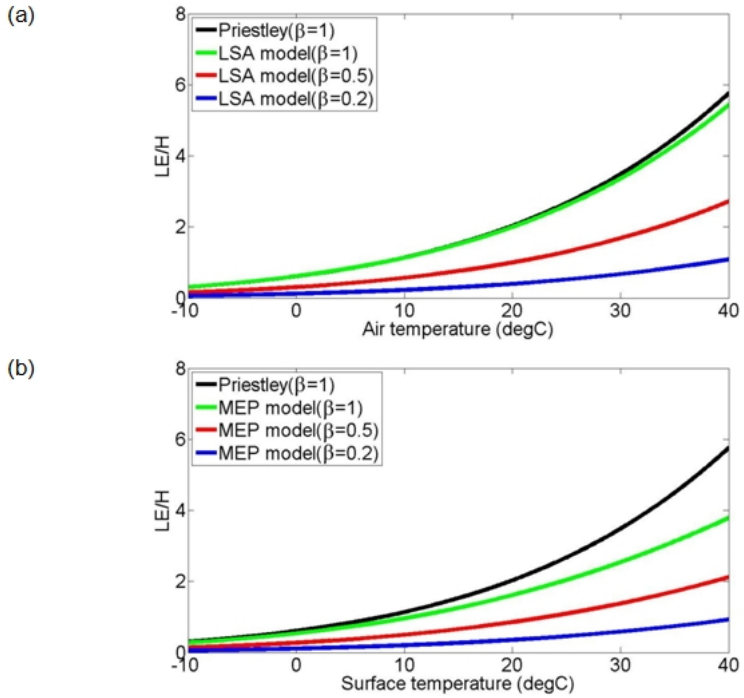

Fig. 2. Model comparison for relative efficiency of *LE* between (a) the LSA and Priestley models, and (b) the MEP and Priestley models

In both LSA and MEP model, the relative efficiency is sensitive to the surface water availability parameter β. For low β values (< 0.2), the relative efficiency increases slightly (LE/H< 1) when temperature increases from -10ºC to 40ºC. While for fully saturated condition (β = 1) the relative efficiency increases more significantly (more than 4 folds) with the same temperature rise. For a given temperature, the evaporation process attains maximum rate when the soil is fully saturated, limited by available energy and the atmospheric demand (Stage I evaporation, see [41] for more details). As β decrease, evaporation becomes limited by water availability at the surface (or more precisely, at the drying front) through soil water transport, such that the actually evaporation decreases rapidly below its potential value (Stage II evaporation). From results in Fig. 2, it is clear that the evaporation rate and the process of latent heat transport are more efficient at higher temperature and wetter surfaces.

3.2 Model Comparison against Field Measurements

Comparisons of the predicted relative efficiency of *LE* by the LSA model and field measurements over the suburban area are shown in Fig. 3. One summer (May to August 2011) and one winter (November 2010 to February 2011) periods were selected to demonstrate the impact of seasonal variability of local climate. Field measurement data

points concentrate in the range of β = 0.05 to 0.3 for the summer period. For the winter period, same trend of data is observed but with larger values of β, ranging from 0.1 to 0.7. As daily mean value is used in the analysis, specific values of β, in general, vary from day to day, but tend to concentrate within certain ranges to reflect the seasonal variability of the surface moisture availability. As shown in Fig. 3, deviations are reasonable with 11.89% and 10.24% of data points outside the predicted range in summer and winter, respectively. Extreme large values from field measurements in both seasons are likely caused by prolonged clouds and rains that reduce available solar energy and suppress sensible heat flux at the surface.

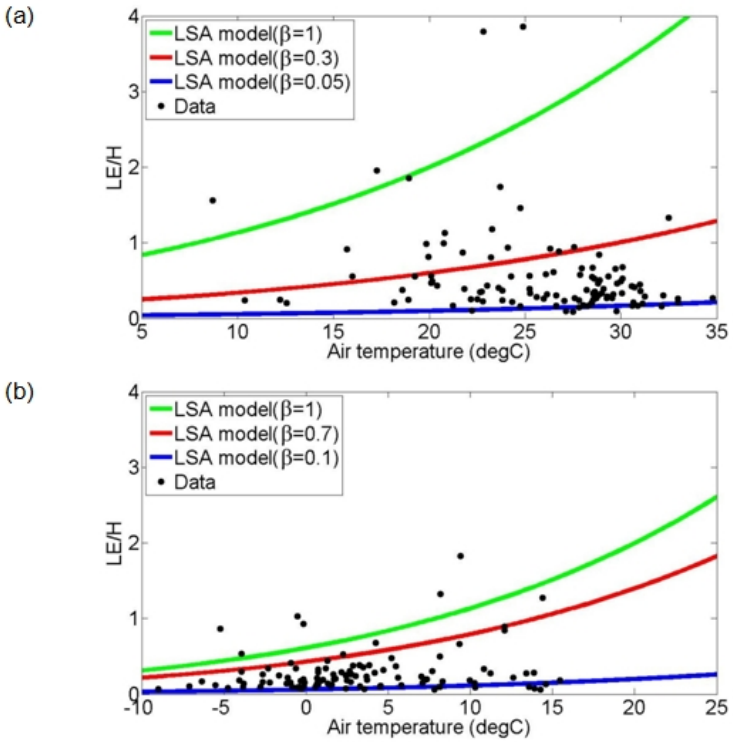

Fig.3. Comparison of the LSA model predictions and field measurements for relative efficiency of *LE* over suburban area, for (a) summer (May to August 2011), and (b) winter (November to February 2011) seasons respectively

Results of comparison between the MEP and Priestley model predictions are shown in Fig. 4. Priestley model overestimates the relative efficiency of *LE* for water-limited land surfaces, as expected. Field datasets are in reasonably good agreement with the MEP model predictions withβ ranging from 0.05 to 0.3 in summer and 0.1 to 0.7 in winter, which is consistent with the LSA model. Compared to LSA model, deviations in MEP model is slightly larger with 15.08% and 11.76% outside the predicted range in summer and winter respectively. The predicted higher efficiency of latent heat transport (thus the evaporation process) in winter is likely due to the snow-melting that continuously wetted and maintain high saturation level of the surface through the season. In addition, snow cover in winter will decrease the temperature difference between the surface and overlying air layer, leading to smaller sensible heat fluxes and eventually larger relative efficiency of *LE*.

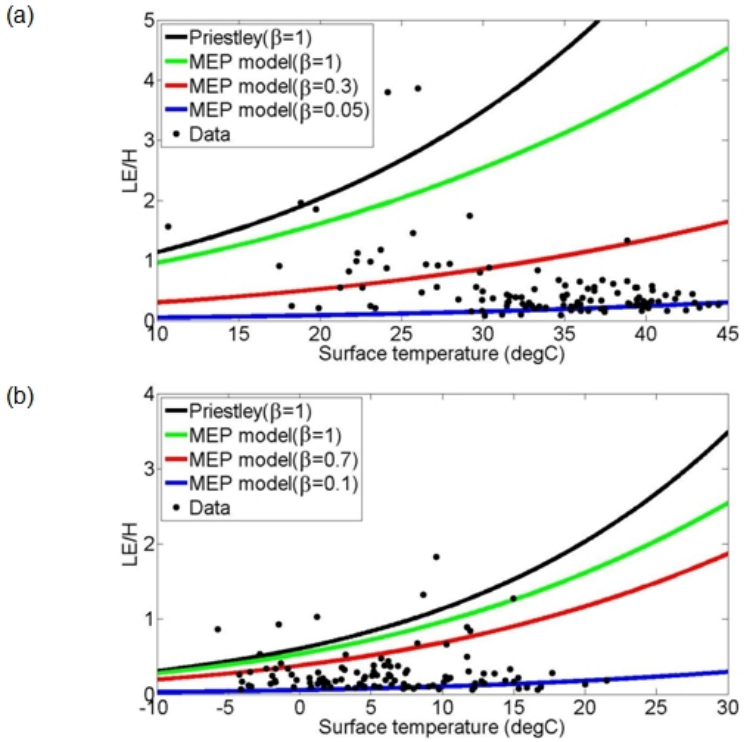

Fig.4. Comparison of Priestley and MEP predictions and field measurements for relative efficiency of *LE* over suburban area, for (a) summer (May to August 2011), and (b) winter (November to February 2011) seasons respectively

Fig. 5 shows comparisons for relative efficiency of *LE* over the lake surface between the LSA model predictions and field measurements. Field measurement data points generally fit in the range of*β* from 0.1 to 0.5. Besides, trends for field measurement at four different heights are similar. A total 16 out of 136 data points fall slightly outside the predicted range. It apparently suggests that, close to the water surface, the measurement height is not playing an important role in affecting the relative efficiency. Over the lake, the surface is fully saturated such that*β* is expected to be close to unity, whereas the predicted*β* range in Fig. 5 is much smaller. This is mainly due to the limitation associated with the theoretical models, in which the efficiency of evaporation is assumed to be dominated by the surface energy partitioning with an unlimited capacity of atmospheric demand. This assumption is valid for land surface with limited surface water availability where the stage II evaporation prevails. Over the lake surface, however, the atmospheric demand determines the actual rate of evaporation. Close to the surface, the atmosphere over a large fetch of water surface is nearly saturated, such that the actual evaporation rate depends on the rate that the water vapor is transported away by wind advection. Thus the parameter*β*,in this case, reflects the efficiency of water vapor advection by wind, rather than the surface water availability as over land surfaces. Similar results of comparison between the MEP model and field measurement are shown in Fig. 6. Due to high heat capacity of water, Fig. 6 has a smaller range of (surface) temperature variation and the increasing trend is not as obvious, as compared to Fig. 5.

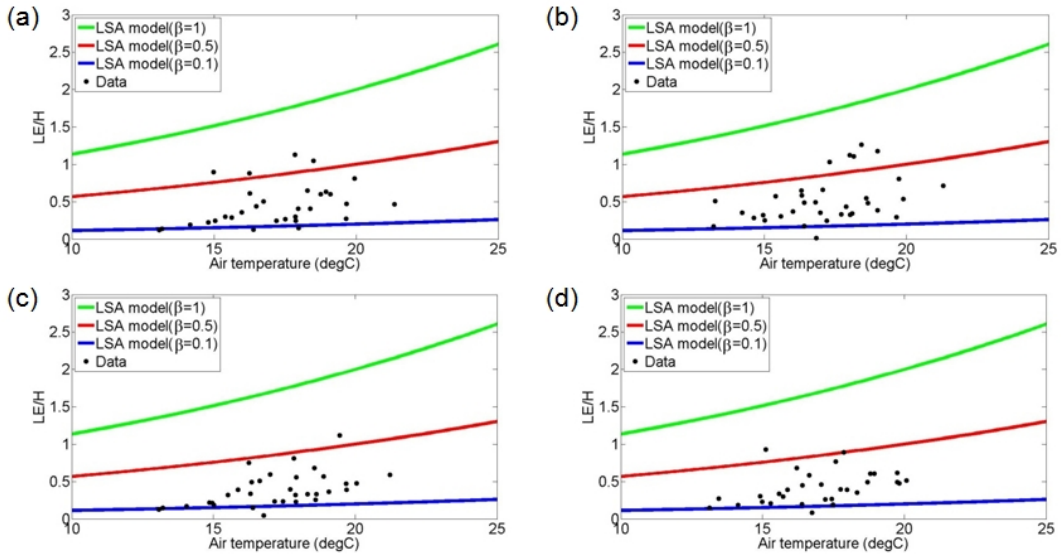

Fig. 5. Comparison for relative efficiency of *LE* over a lake surface between LSA predictions and field measurements at height (a) H = 1.66m, (b) H = 2.31m, (c) H = 2.96m, and (d) H=3.61m, respectively

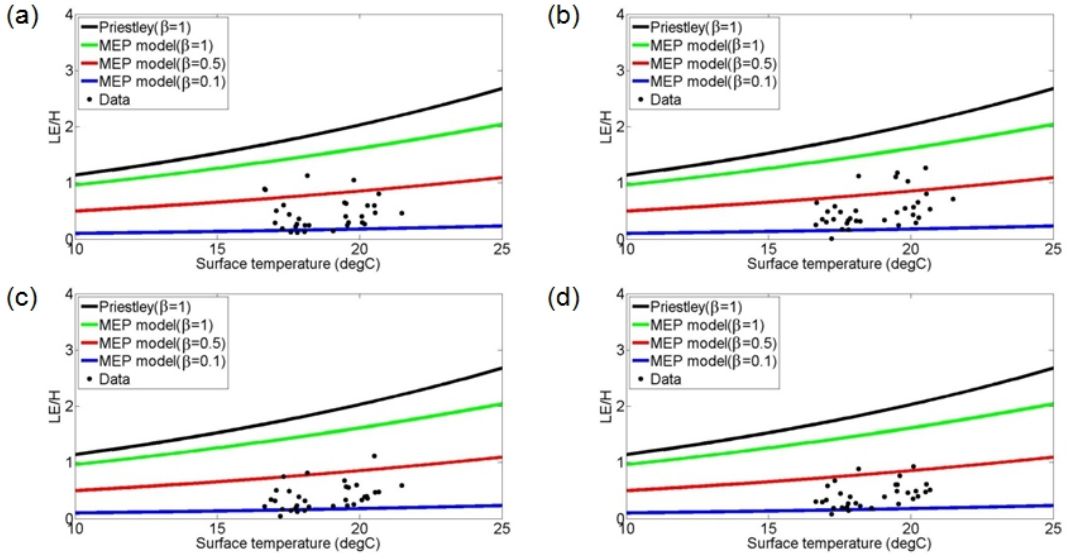

Fig. 6. Comparison for relative efficiency of *LE* over a lake surface between Priestley and MEP predictions and field measurements at height (a) H = 1.66m, (b) H = 2.31m, (c) H = 2.96m, and (d) H=3.61m, respectively

Over the grassland, comparisons between the LSA model predictions and field measurements are plotted for different months in Fig. 7. In September 2010, field data points fit in model prediction with *β* ranging from 0.2 to 0.5, whereas for the other two months, data points fall largely out of the physical range of*β*. The underestimation of latent heat transport in the LSA model is largely due to the lack of physical resolution of the transpiration process

in the model. In May and June, grasses at the experimental site underwent rapid growing and the root uptake of water contributes a significant fraction to the total latent heat arising from the grassland due to transpiration process. Since the LSA model only accounts for pure evaporation from the surface, it is not surprising that the model consistently underestimates the actual latent heat (due to evapotranspiration) during the growing season of vegetated surfaces.

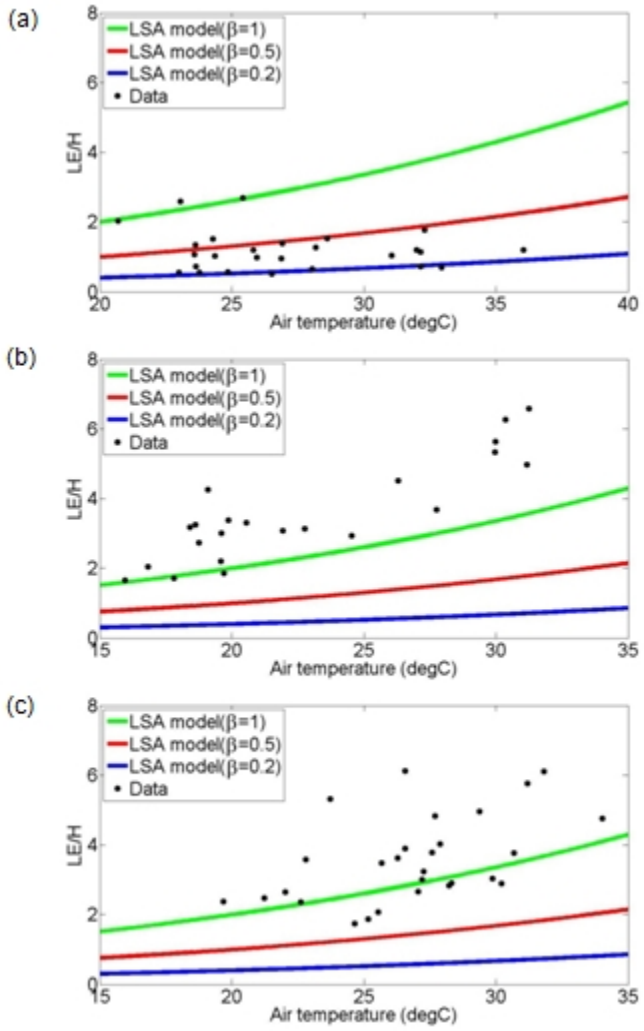

Fig. 7. Comparison for relative efficiency of *LE* over a grassland surface between LSA predictions and field measurements for (a) September 2010, (b) May 2011, and (c) June 2011, respectively

In contrast, as discussed in Section 2, the MEP model is capable of resolving the transpiration process by considering thermodynamic conditions at leaf surfaces instead of the land surface. For the grassland dataset available, field measurements of leaf temperature were missing. To demonstrate the contribution of transpiration to total latent heat, we resort to empirical relations reported in the literature. Under strong radiative

exposure (convective atmospheric surface layer), the difference between the air and leaf temperature varies approximately from 3ºC to 16ºC for thin leaf plants [42,43]. Here we adopt an average temperature difference of 5ºC between grass leaf and the overlying atmosphere, for the purpose of illustration the performance of the MEP model with incorporated transpiration process. Results of comparison between the MEP predictions and field measurements are shown in Fig. 8.

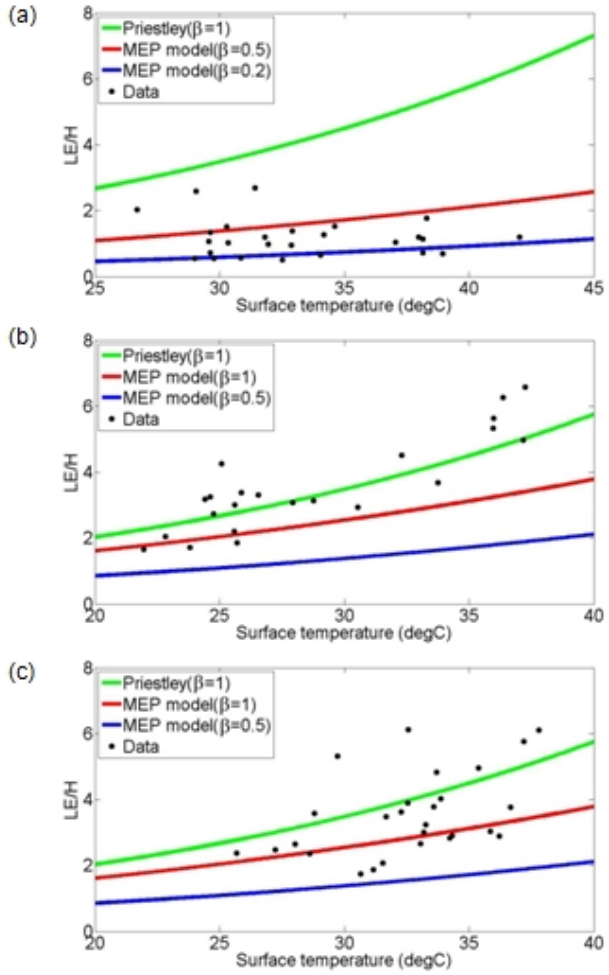

Fig. 8. Comparison for relative efficiency of *LE* over a grassland surface between Priestley and MEP predictions and field measurements for (a) September 2010, (b) May 2011, and (c) June 2011, respectively

With the incorporation of the transpiration process, the relative efficiency of latent heat predicted by the MEP is clearly in more reasonable agreement with field measurements, particular in May and June (Fig. 8b and 8c). Thus to fully utilize the strength of the MEP model when applied to vegetated surfaces, the leaf temperature needs to measured separately from the land (soil) surface temperature, and a two source energy transport model is preferred to account the evaporation and transpiration processes separately [44].

4. CONCLUSION

The relation between turbulent fluxes in the surface energy budget can be expressed in terms of the relative efficiency. In this study, three theoretical models for relative efficiency predictions based on different mechanisms were intercompared and evaluated using experimental measurements. For applications to land surfaces with limited surface moisture availability, water availability parameter β is incorporated into the MEP model in this study. Results show that β is a critical parameter for regulating the actual evolutional trends of relative efficiency with temperature variation. The incorporation of β parameter enables the LSA and MEP models for predicting the actual evaporation efficiency, over a wide range of realistic land cover types with limited water availability. The conventional Priestley model, on the other hand, provides an upper bound of the relative efficiency of latent heat over the saturated surface. All model predictions of the relative efficiency show an increasing trend of latent heat transport with scaling temperatures (air temperature in the LSA model and LST in Priestley and MEP models).

Comparing against datasets obtained using field measurements, the LSA and MEP models predicted the relative efficiency with similar β ranges over the lake surface and the suburban area. The parameter β, scaling from 0 to unity, represents the physical constraint of evapotranspiration due to either the availability of water over land surfaces or the efficiency of water vapor advection over large water surfaces. For vegetated surfaces, while only evaporation is accounted, the LSA model consistently underestimates the efficiency of latent heat transport, resulting $\beta > 1$ for measured datasets especially during the growing season of vegetation. Incorporation of the transpiration process in the MEP model significantly improves the model performance by bringing β to the physical range.

Lastly, it is noteworthy that all three theoretical models discussed in this study are based on the surface energy balance given in Eq. (1). In comparison to field measurements by EC towers, we omitted the fact that the sum of total turbulent heat fluxes ($H + LE$) in field measurements usually underestimate the available energy ($R_n - G$) over long time scales, leaving an energy residual (up to 30% of the available energy) unexplained by the SEB equation. This is known as the surface energy imbalance closure problem [45,46,47]. The magnitude of the energy residual is significant such that its re-partitioning can largely affect the actual magnitude and the relative distribution of all dissipative energy budgets in measurement datasets. Up to date, the surface energy closure problem remains outstanding [48] and needs to be addressed in future investigations.

ACKNOWLEDGEMENTS

This work is partly supported by the Arizona Salt River Project (SRP) under account XAS0330. The authors would like to thank the following personnel for sharing field measurement datasets: Professor Marc Parlange and the rest of the Environmental Fluid Mechanics and Hydrology Laboratory at the Swiss Federal Institute of Technology—Lausanne (EPFL) for the lake dataset; Professor Elie Bou-Zeid and the rest of the Environmental Fluid Mechanics Group at Princeton University for the suburban dataset; and Professor James Smith, Dr. Mary-Lynn Baeck and the rest of the Hydrometeorology Research Group at Princeton University for the grass field dataset.

COMPETING INTERESTS

Authors have declared that no competing interests exist.

REFERENCES

1. IPCC. Climate change 2007: The physical science basis. Contribution of working group I to the fourth assessment report of the intergovernmental panel on climate change. New York: Cambridge University Press; 2007.
2. Cook ER, Woodhouse CA, Eakin CM, Meko DM, Stahle DW. Long-term aridity changes in the western United States. Science. 2004;306(5698):1015-1018. doi:10.1126/science.1102586.
3. Pall P, Aina T, Stone DA, Stott PA, Nozawa T, Hilberts AGJ, et al. Anthropogenic greenhouse gas contribution to flood risk in England and Wales in autumn 2000. Nature. 2011;470(7334):382-385. doi:10.1038/nature09762.
4. Lin N, Emanuel K, Oppenheimer M, Vanmarcke E. Physically based assessment of hurricane surge threat under climate change. Nature Clim Change. 2012;2(6):462-467. doi:10.1038/nclimate1389.
5. Sellers PJ, Dickinson RE, Randall DA, Betts AK, Hall FG, Berry JA, et al. Modeling the exchanges of energy, water, and carbon between continents and the atmosphere. Science. 1997;275(5299):502-509. doi:10.1126/science.275.5299.502.
6. Seneviratne SI, Luthi D, Litschi M, Schar C. Land-atmosphere coupling and climate change in Europe. Nature. 2006;443(7108):205-209. doi:10.1038/nature05095.
7. Katul GG, Oren R, Manzoni S, Higgins C, Parlange MB. Evapotranspiration: A process driving mass transport and energy exchange in the soil-plant-atmosphere-climate system. Rev Geophys. 2012;50:RG3002. doi:10.1029/2011RG00366.
8. McCumber MC, Pielke RA. Simulation of the effects of surface fluxes of heat and moisture in a mesoscale numerical model. 1. Soil Layer. J Geophys Res-Ocean Atmos. 1981;86(Nc10):9929–9938. doi:10.1029/JC086iC10p09929.
9. Chen F, Dudhia J. Coupling an advanced land surface-hydrology model with the Penn State-NCAR MM5 modeling system. Part I: Model implementation and sensitivity. Mon Weather Rev. 2001;129(4):569–585.
10. Wood EF, Sivapalan M, Beven K, Band L. Effects of spatial variability and scales with implications to hydrological modeling. J Hydrol. 1988;102:29-47. doi:10.1016/0022-1694(88)90090-X.
11. Salmond JA, Roth M, Oke TR, Christen A, Voogt JA. Can surface cover tiles be summed to give neighborhood fluxes in cities? J Appl Meteorol Climatol. 2012;51(1):133-149. doi:10.1175/JAMC-D-11-078.1.
12. Moran MS, Kustas WP, Vidal A, Stannard DI, Blanford JH, Nichols WD. Use of ground-based remotely sensed data for surface energy balance evaluation of a semiarid rangeland. Water Resour Res. 1994;30(5):1339-1349. doi:10.1029/93WR03064.
13. Sandholt I, Rasmussen K, Andersen J. A simple interpretation of the surface temperature/vegetation index space for assessment of surface moisture status. Remote Sens Environ. 2002;79:213–224. doi:10.1016/S0034-4257(01)00274-7.
14. Kalma JD, McVicar TR, McCabe MF. Estimating land surface evaporation: A review of methods using remotely sensed surface temperature data. Surv Geophys. 2008;29:421–469. doi:10.1007/s10712-008-9037-z.

15. Anderson MC, Norman JM, Diak GR, Kustas WP, Mecikalski JR. A two-source time-integrated model for estimating surface fluxes using thermal infrared remote sensing. Remote Sens Environ. 1997;60(2):195–216. doi:10.1016/S0034-4257(96)00215-5.
16. Mecikalski JR. Estimating fluxes on continental scales using remotely sensed data in an atmospheric-land exchange model. J Appl Meteorol. 1999;38(9):1352–1369.
17. Jiang L, Islam S. Estimation of surface evaporation map over Southern Great Plains using remote sensing data. Water Resour Res. 2001;37(2):329-340. doi:10.1029/2000WR900255.
18. Biltoft CA, Pardyjak ER. Spectral coherence and the statistical significance of turbulent flux computations. J Atmos Ocean Tech. 2009;26(2):403-410. doi:10.1175/2008JTECHA1141.1.
19. Ramamurthy P, Pardyjak ER. Toward understanding the behavior of carbon dioxide and surface energy fluxes in the urbanized semi-arid Salt Lake Valley, Utah, USA. Atmos Environ. 2011;45(1):73-84. doi:10.1016/j.atmosenv.2010.09.049.
20. Wang ZH, Bou-Zeid E, Smith JA. A coupled energy transport and hydrological model for urban canopies evaluated using a wireless sensor network. Q J R Meteorol Soc. 2013; *(in press).*doi:10.1002/qj2032.
21. Bowen IS. The ratio of heat losses by conduction and by evaporation from any water surface. Phys Rev. 1926;27:779–787. doi:10.1103/PhysRev.27.779.
22. Priestley CHB. Turbulent transfer in the lower atmosphere. Chicago: University of Chicago Press; 1959.
23. Wang J, Bras RL. A model of surface heat fluxes based on the theory of maximum entropy production. Water Resour Res. 2009;45:W11422. doi:10.1029/2009WR007900.
24. Wang J, Bras RL. A model of evapotranspiration based on the theory of maximum entropy production. Water Resour Res. 2011;47:W03521. doi:10.1029/2010WR009392.
25. Bateni SM, Entekhabi D. Relative efficiency of land surface energy balance components. Water Resour Res. 2012;48:W04510. doi:10.1029/2011WR011357.
26. Bhumralkar CM. Numerical experiment on computation of ground surface temperature in an atmospheric general circulation model. J Appl Meteorol. 1975;14(7):1246-1258.
27. Gao Z, Horton R, Wang L, Liu H, Wen J. An improved force-restore method for soil temperature prediction. Eur J Soil Sci. 2008;59(5):972-981.doi:10.1111/j.1365-2389.2008.01060.x.
28. List RJ. Smithsonian meteorological tables. Washington, DC: Smithsonian Institute Press; 1984.
29. Elliott WP, Gaffen DJ. Effects of conversion algorithms on reported upper air dewpoint depressions. Bull Am Meteorol Soc. 1993;74:1323-1325.
30. Jaynes ET, Bretthorst GL. Probability theory – the logic of sciences. New York: Cambridge University Press; 1993.
31. Ozawa H, Ohmura A, Lorenz RD, Pujol T. The second law of thermodynamics and the global climate system: A review of the maximum entropy production principle. Rev Geophys. 2003;41:4/1018. doi:10.1029/2002RG000113.
32. Dewar RC. Maximum entropy production and the fluctuation theorem. J Phys A Math Gen. 2005;38:L371-L381. doi:10.1088/0305-4470/38/21/L01.
33. Vercauteren N, Bou-Zeid E, Parlange MB, Lemmin U, Huwald H, Selker JS, et al. Subgrid-scale dynamics of water vapour, heat, and momentum over a lake. Boundary-Layer Meteorol. 2008;128(2):205–228. doi:10.1007/s10546-008-9287-9.
34. Vercauteren N, Huwald H, Bou-Zeid E, Selker JS, Lemmin U, Parlange MB, et al. Evolution of superficial lake water temperature profile under diurnal radiative forcing. Water Resour Res. 2011;47:W09522. doi:10.1029/2011WR010529.

35. Wang ZH, Bou-Zeid E. A novel approach for the estimation of soil ground heat flux. Agric For Meteorol. 2012;154-155:214-221. doi:10.1016/j.agrformet.2011.12.001.
36. Wang ZH. Reconstruction of soil thermal field from a single depth measurement. J Hydrol. 2012;464-465:541-549. doi:10.1016/j.hydrol.2012.07.047.
37. Wang ZH, Bou-Zeid E, Smith JA. A spatially-analytical scheme for surface temperatures and conductive heat fluxes in urban canopy models. Boundary-Layer Meteorol. 2011;138(2):171-193. doi:10.1007/s10546-010-9552-6.
38. Wilczak JM, Oncley SP, Stage ST. Sonic Anemometer tilt correction algorithms. Boundary-layer Meteorol. 2001;99:127-150. doi:10.1023/A:1018966204465.
39. Webb EK, Pearman GI, Leuning R. Correction of flux measurements for density effects due to heat and water vapor transfer. Q J R Meteorol Soc. 1980;106:85–100. doi:10.1002/qj.49710644707.
40. Stull RB. An introduction to boundary layer meteorology. Dordrecht: Kluwer Academic; 1988.
41. Shokri N, Lehmann P, Vontobel P, Or D. Drying front and water content dynamics during evaporation from sand delineated by neutron radiography. Water Resour Res. 2008;44(6):W06418. doi:10.1029/2007WR006385.
42. Linacre ET. A note on a feature of leaf and air temperatures. Agricul Meteorol. 1964;1(1):66-72. doi:10.1016/0002-1571(64)90009-3.
43. Noffsinger TL. Leaf and air temperatures under Hawaii conditions. Pacific Sci. 1961;15:304-306.
44. Kustas WP, Norman JM. Evaluation of soil and vegetation heat flux predictions using a simple two-source model with radiometric temperatures for partial canopy cover. Agric For Meteorol. 1999;94(1):13-29.
45. Foken T. The energy balance closure problem: an overview. Ecol Appl. 2008;18(6):1351–1367. doi:10.1890/06-0922.1.
46. Leuning R, Gorsel EV, Massman WJ, Isaac PR. Reflections on the surface energy imbalance problem. Agric For Meteorol. 2012;156:65-74. doi:10.1016/j.agrformet. 2011.12.002.
47. Wilson K, Goldstein A, Falge E, Aubinet M, Baldocchi D, Berbigier P, et al. Energy balance closure at FLUXNET sites. Agric For Meteorol. 2002;113 (1-4):223–243. doi:10.1016/S0168-1923(02)00109-0.
48. Wohlfahrt G, Widmoser P. Can an energy balance model provide additional constraints on how to close the energy imbalance? Agric For Meteorol. 2013;169:85-91. doi:10.1016/j.agrformet.2012.10.006.

Peer-review history:
The peer review history for this paper can be accessed here:
http://www.sciencedomain.org/review-history.php?iid=218&id=10&aid=1221